JOURNAL OF MATERIALS SCIENCE **35** (2000) 931–936

Characterization and size-dependent magnetic properties of $Ba_3Co_2Fe_{24}O_{41}$ nanocrystals synthesized through a sol-gel method

GANG XIONG*, GUOBAO WEI, XUJIE YANG, LUDE LU, XIN WANG‡
Materials Chemistry Laboratory, Nanjing University of Science and Technology, Nanjing 210094, People's Republic of China
E-mail: wxin@public1.ptt.js.cn

$Ba_3Co_2Fe_{24}O_{41}$ nanocrystals are synthesized through a stearic acid sol-gel method. The reaction temperatures are dramatically lower than that of the conventional ceramic method. The nanocrystalline powders obtained at 750 °C were spherical in shape with grain sizes in the range 15–25 nm and become a plate-like form when the heat-treatment temperature increased. The magnetic properties of these samples are different from those of the bulk Z-type hexagonal ferrite with a lower specific saturation magnetization. This phenomenon can be attributed to the existing of a nonmagnetic layer existing on the surface of the particles. The higher value of the coercivity force is obtained when the particle sizes approximately are equal to 90 nm and assume a single-domain character. The surface composition of the nanocrystalline Co_2-Z hexagonal ferrite is different from that of the bulk counterpart material with a higher content of the Ba element and Co element.

1. Introduction

Inspired by the realization that the physicochemical properties of nanophase materials are dramatically different from those of the bulk counterparts and usually exhibit new or crossover phenomena, the design, preparation and characterization of nano-materials have been of great interest [1, 2]. Ultrafine magnetic particles, for example, exhibit unique phenomena such as superparamagnetism and quantum tunneling of magnetization. Below a critical size, magnetic particles become single domain as opposed to multidomain in the bulk materials and can possess unusually high coercivities [3–5]. Because of their unique physical properties, nano-scale magnetic particles have high potential for applications in diverse areas such as high density perpendicular recording, color imaging, ferrofluids, UHF (ultra-high frequency: 300 MHz to 3 GHz) devices and magnetic refrigeration [6–8]. During the past few years, the ultrafine hexagonal ferrites have been the subject of intense research. Several synthesis procedures have been proposed up to now to obtain ultrafine particles of hexagonal crystal system ferrite: the glass-crystallization method [9, 10], hydrothermal synthesis method [11], chemical coprecipitation method [12, 13], organic resin method [14], microemulsion mediated process [15, 16] and the so-called liquid mix technique [17, 18]. Almost all studies, however, have been focused merely on the synthesis and magnetic properties of M-type and W-type hexagonal crystal system ultrafine particles. Other types of hexagonal crystal system ferrite ultrafine particles (such as X-, Y-, Z- and U-type) can not conveniently synthesized by these methods mentioned above because of their more complicated structures. These materials are usually been prepared by the ceramic method. High calcination temperatures (1100–1400 °C) are applied for the solid reaction to occur and often result in the formation of coarse aggregation. The sizes of the powders so produced are larger than 0.5 μm. There are few papers dealing with the preparation and magnetic properties of these kinds of hexagonal ferrite nanocrystals and the full range of exploitation of the potential offered by these materials is strongly limited.

In our earlier works, we have developed a relatively novel non-aqueous synthesis method—the stearic acid gel method for the preparation of M-type and W-type hexagonal crystal system ferrite nanocrystals and the final powders with size of 10–200 nm were obtained [19, 20]. The main advantage of this technique is that the raw materials are mixed on an atomic level in the liquid state and the temperature of solid state reaction is lowered obviously. The composition of the final product also can be accurately controlled. These merits make it distinguished from other methods, especially for the preparation of multicomponent composite oxides.

Z-type (Co_2-Z) hexagonal crystal system ferrite nanocrystals have now been prepared through the stearic

* *Present address*: Institute of Physics & Center for Condensed Matter Physics, Chinese Academy of Sciences, Beijing 100080, China.
‡ Author to whom all correspondence should be addressed.

acid gel method. We report here an investigation of the morphological, structural, magnetic and surface compositional characteristic of the products which has been carried out by means of x-ray powder diffraction (XRD), transmission electron microscope (TEM), vibrating sample magnetor (VSM) and x-ray photoelectron spectroscope(XPS). The influences of the particle size effect on the magnetic properties of the products also are researched. Further results concerning other kinds of hexagonal crystal system ferrite nanocrystals such as X-type, Y-type and U-type is still under way and will be reported elsewhere in the future.

2. Experimental details

2.1. Synthesis

The raw materials utilized in the present study were barium hydrate purchased from Yuelong Chemical Factory in Shanghai, Cobalt acetate bought from Hailing Chemical Factory in Nanjing, ferric nitrate supplied by Nanjing Chemical Factory and stearic acid purchased from the Second Reagent Factory of Shanghai, all of analytically pure. These materials were weighed with molar ratios of Co : Ba : Fe equal to 2 : 3 : 24. The synthesis procedures were as follows: an appropriate amount of stearic acid was heated and melted, and then the weighed barium hydrate, cobalt acetate and ferric nitrate were added into it. After complete mixing, the solution was heated at 80–100 °C for about 2 h and obtained a homogeneous transparent solution sol. The sol was slowly cooled to ambient temperature and formed a gel. Finally, the gel precursor was calcined at 450 °C for 0.5 h and subsequently heat-treated 650 °C, 750 °C, 850 °C, 950 °C, 1050 °C, 1150 °C respectively, to obtain loose black powders.

2.2. Characterization

The identification of the crystalline phases of these samples appearing after the heat-treatment is carried out on a Rigaku D/MAX—III X-ray powder diffractometer operating at 40 KV and using Cu K_α radiation. Transmission electron micrographs (TEM) were taken with a JEM-200CX microscope operating at 150 KV. The specific surface areas were measured by the Brunauer-Emmett-Teller (BET) method at liquid nitrogen temperature using N_2 gas as the adsorbent and samples were degassed at 300 °C for 6 hours prior to analysis. Saturation magnetization σ_s and coercivity H_c were measured at room temperature using a LDJ-9500 vibrating sample magnetometer (VSM) with maximum applied field of 6.37×10^5 Am^{-1}. Saturation magnetization σ_s was obtained by a $1/H^2$ extrapolation to the infinite field. X-ray photoelectron spectroscope (XPS) analysis was performed using a Perkin-Elmer PHI ESCA 5300 spectrometer with a Mg K (1253.6 eV) achromatic X-ray source operated at 15 KeV and an emission current of 20 mA. The vacuum inside the analysis chamber was maintained at $<2 \times 10^{-7}$ Torr during the analysis. Samples with a dimension of 1 cm × 1 cm were mounted on the sample holder with double-sided tape. Analysis were obtained for the center area of 2×2 mm^2. All samples used for XPS measurements were single-crystal silicon substrates and were analyzed at ambient temperature.

3. Results and discussion

3.1. XRD

The X-ray diffraction patterns of the heat-treated powders indicated that, at heat-treating temperature up to 650 °C, the sample was mainly consisted of γ-Fe_2O_3 and $BaCO_3$. Z-type ($Ba_3Co_2Fe_{24}O_{41}$) hexagonal crystal system ferrite powders were then obtained when heat-treating temperature raised above 750 °C. XRD patterns of the specimens subjected to different heat-treatment temperature were recorded and the results are shown in Fig. 1. The broadening of diffraction lines are caused by the small crystalline size effect of the samples. With the increase of the calcination temperature the grain sizes increased and the diffraction line became narrow.

The average grain sizes were first determined from the XRD pattern parameters of the specimens according to the Scherrer equation [21]:

$$D = \frac{k\lambda}{(\beta \cos\theta)}$$

where D is the average grain size, k is a constant equal to 0.89, λ is the X-ray wavelength equal to 0.1542 nm, β is the full width at half-maximum (FWHM) and θ is the diffraction angle. The results obtained are shown in Table I. It can be seen that the grain size grows with the increase of the heat-treating temperature.

3.2. TEM and EDP

The morphology of nanocrystalline Z-type hexagonal ferrite heat-treated at various temperatures was studied by transmission electron microscopy (TEM) and the results are shown in Fig. 2. It can be seen that particles heat treated at 750 °C are spherical, of uniform size and with the grain sizes in the range 15–25 nm. Fig. 2b indicated that the morphology of the powders obtained at 850 °C changed to plate from and the grain sizes in the range 40–60 nm. The average grain sizes of the specimen determined by statistics mean method are also listed in Table I. It can seen that the outcomes are basically consistent with that of the XRD method.

Fig. 3 shows the electron diffraction pattern of nanocrystalline Z-type hexagonal system ferrite. It can be seen that the patterns of specimen heat treated at 750 °C were some closed circles and the patterns of the specimen obtained at 850 °C were some uncontinuous bright spots. This phenomenon also can be attributed to the

TABLE I Average grain sizes determined from XRD pattern using the Scherrer equation and TEM

Temperature (°C)	750	850	950	1050	1150
d_{XRD} (nm)	26.3	61.3	86.6	136	210
d_{TEM} (nm)	23.4	52.0	76.1	120	180

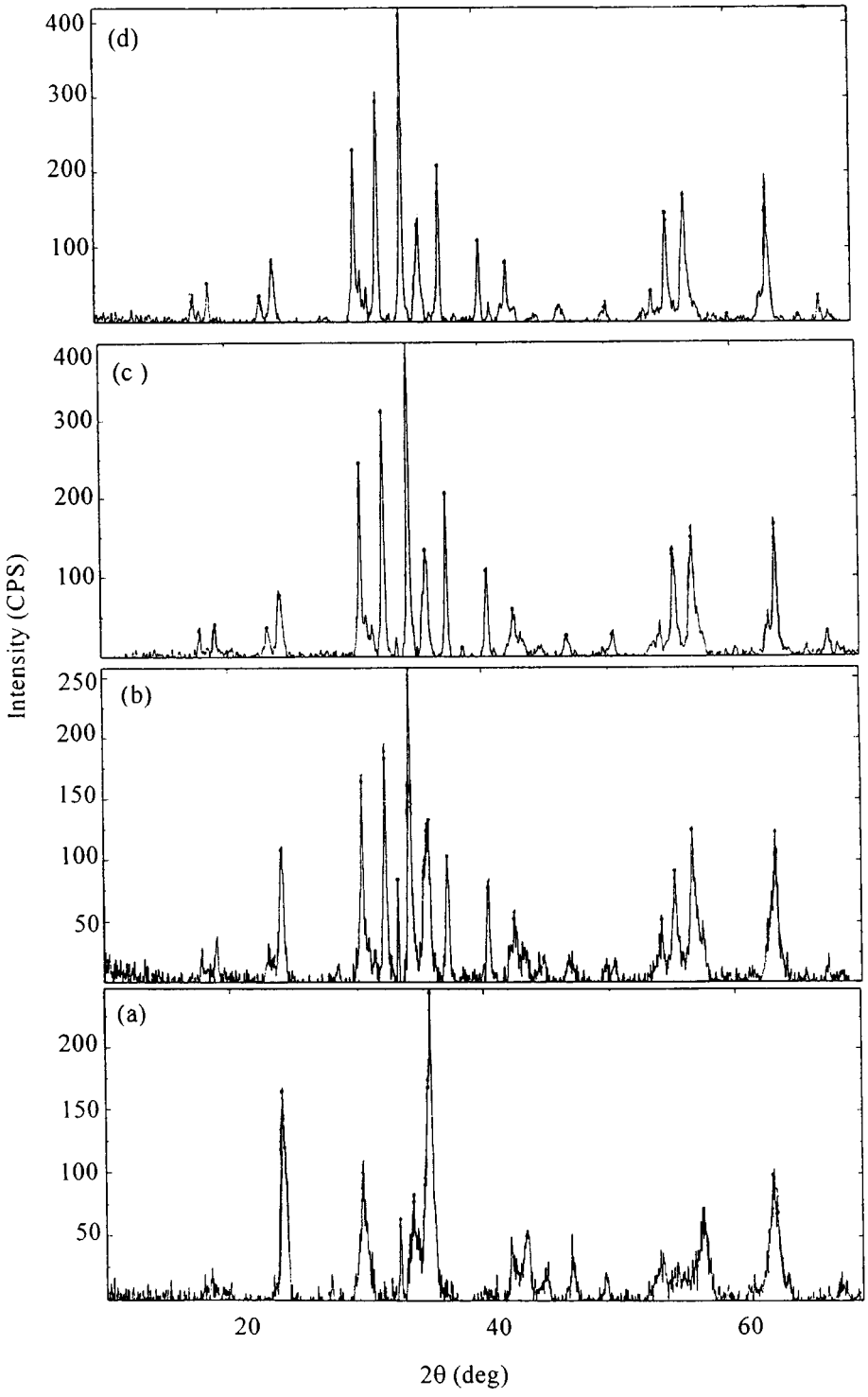

Figure 1 XRD patterns of the nanocrystalline Co_2-Z type hexagonal ferrite powders calcined at different temperature. (a) 650 °C (b) 750 °C (c) 850 °C (d) 950 °C.

small crystalline size effect. With the decrease of the grain size the number of diffraction spots is increased. Below a critical size the pattern would become a series of closed circles and differentiated from that of the bulk counterpart. It is also one of the unique features of nanophase-materials.

3.3. BET

The specific surface areas of the powders gained at different temperatures were measured by the BET method at liquid-nitrogen temperature (N_2 adsorption) and the average grain size, d (nm), can be calculated according to the following equation:

$$d = 6 \times \frac{10^6}{(S\rho)}$$

where S (m^2/g) is the specific surface area of the particles and ρ is the density of Z-type (Co_2-Z) hexagonal crystal system ferrite and equal to 5.33×10^3 kg/m^3. The results including the determined specific surface areas and the deduced average grain sizes of the specimens heat treated at various temperatures are listed in Table II.

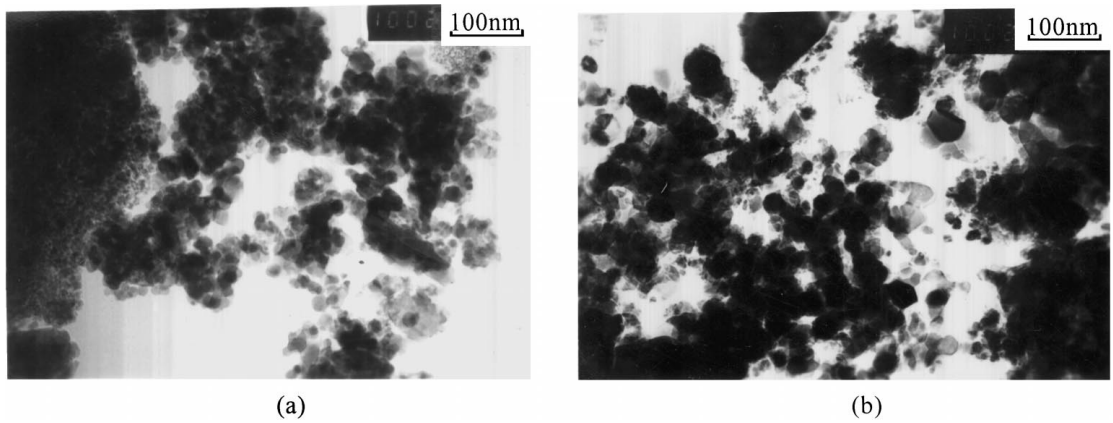

Figure 2 TEM micrographs of Co_2-Z type hexagonal ferrite nanocrystals calcined at different temperatures (a) 750 °C (b) 850 °C.

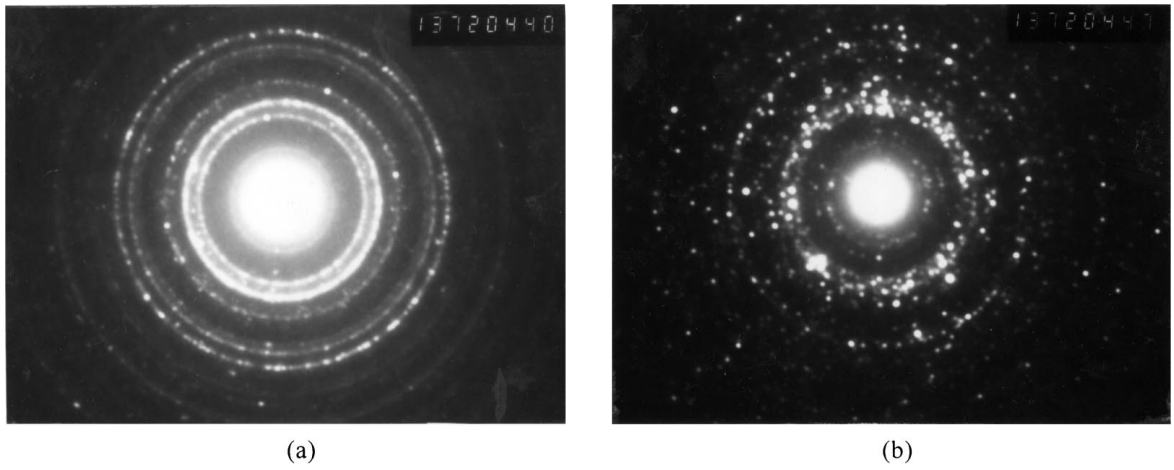

Figure 3 Electron diffraction pattern of Co_2-Z type hexagonal ferrite nanocrystals calcined at different temperatures (a) 750 °C (b) 850 °C.

TABLE II Specific surface areas and the average grain sizes determined by the BET method

Temperature (°C)	750	850	950	1050	1150
S (m^2/g)	35.7	15.5	11.9	7.4	4.7
d (nm)	31.5	72.7	94.5	152	240

On comparison of the results on the grain size determined by the three characterization methods, i.e., XRD , TEM and the BET method, it can be found that the grain sizes estimated by the specific surface area method were slightly larger than those of the others. This was believed to be the result of agglomeration of the nanocrystals owing to the high surface energy of the ultrafine particles. The adsorptive capacity of N_2 decreased with gathering of the powders and the specific surface area thus determined is smaller than the actual value, so the particle size calculated through the foregoing equation is larger [22].

3.4. XPS

With the decrease of the particle size, the number of the broken bonds on the surface of the particles would increase and the surface composition of the ultrafine particles should be different from that of the bulk counterpart materials. X-ray photoelectron spectroscope is an ideal instrument for the surface analysis because of its high sensitivity and nondestructive nature. The results of surface analysis of Z-type hexagonal ferrite nanocrystals determined by the XPS are listed in Table III. It can be seen that the content of the Ba element and Co element increased with the decrease of the heat-treatment temperature and the particle size, while for Fe element the reverse result was obtained. It also should be noted that the content of the O element did not show any regular changing when the particle size decreased.

TABLE III Surface composition of the samples heat-treated at different temperatures

Heat-treatment temperature (°C)	Ba (%)	Co (%)	Fe (%)	O (%)
750	5.91	16.94	18.31	58.84
850	5.64	15.87	18.73	59.76
950	5.35	15.26	19.02	60.37
1050	5.09	14.96	19.44	60.51
1150	4.95	12.84	22.90	59.31
Bulk Co_2-Z ferrite	4.29	2.86	34.29	58.57

3.5. VSM

Saturation magnetization σ_s of nanocrystalline Z-type hexagonal ferrite was observed to decrease with decreasing particle size. This fact can clearly be seen by

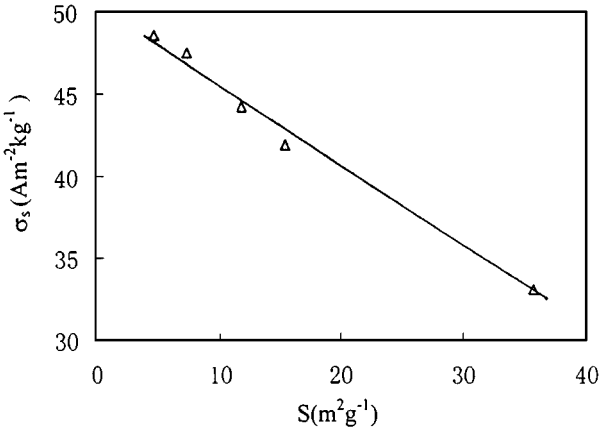

Figure 4 Saturation magnetization of Co_2-Z type hexagonal ferrite nanocrystals as a function of specific surface area.

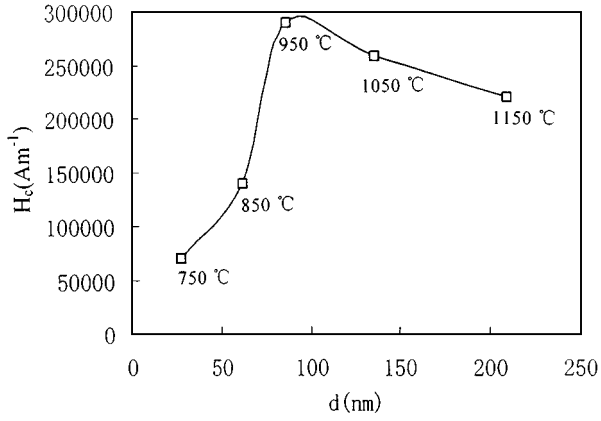

Figure 5 Coercivity of Co_2-Z type hexagonal ferrite nanocrystals as a function of particle size.

plotting σ_s as a function of BET specific surface area S of the particles, as shown in Fig. 4. The figure shows that σ_s decreases linearly as S increases. The result can be explained by assuming a nonmagnetic layer existing on the surface of the particles. In this case, σ_s can be written as

$$\sigma_s = \sigma_0(1 - \delta S\rho),$$

where ρ is the density, δ is the thickness of the nonmagnetic layer and σ_0 is the saturation magnetization for the bulk material. The value of δ, estimated by fitting the experimental results into the above equation, is as small as several angstroms. The decrease in σ_s with decreasing particle size can thus be interpreted as a result of the increase in the ratio of nonmagnetic volume to the total volume of the particles. A similar description of surface nonmagnetic layer effect on the M-type hexagonal ferrite has also been proposed by O. Kubo *et al.* [23].

The variation of coercivity H_c with the heat-treated temperature and thus the corresponding grain size of the Z-type ferrite nanoscale particles is shown in Fig. 5. The samples heated around 950 °C to 1050 °C exhibit higher H_c values thus indicating that at these temperatures the particles appear to assume an increasingly single-domain character. The higher values also result from the orientation of the defect-free single-domain particles obtainable by the sol-gel process. Orientation may occur during sintering of the fine particles.

It is observed from Fig. 5. that, when the specimens are heat-treated at 950 °C and 1050 °C coercivity values of 2.90×10^5 Am^{-1} and 2.59×10^5 Am^{-1} are obtained, respectively. Above 1050 °C the samples exhibited a decrease in value of the coercive force. Undoubtedly the particle distributions are beginning to shift into the multidomain region. According to Herzer theory [24], the coercivity of ferromagnetic particles is in inverse proportion to the grain size d when the particle size exceeding the single-domain size but in direct proportion to d^6 when the particle size is smaller than the single-domain size. The decrease in H_c beyond 1050 °C thus can be attributed to particles exceeding the critical domain size due to sintering. The single-domain size of Co_2-Z hexagonal ferrite, deduced by fitting the experiment result into the Herzer theory, is approximately as big as 90 nm.

4. Conclusion

The stearic acid sol-gel method seems to be a convenient and versatile one for obtained very homogeneous nanoscale Z-type hexagonal ferrite powders. The reaction temperatures are dramatically lower than that of the conventional ceramic method. The nanocrystalline powders obtained at 750 °C were spherical in shape with grain sizes in the range 15–25 nm and become a plate-like from when the heat-treatment temperature increased. The surface composition of the nanocrystalline Co_2-Z hexagonal ferrite is different from that of the bulk counterpart material with a higher content of the Ba element and Co element. The magnetic properties of these samples are different from those of the bulk Z-type hexagonal ferrite with a lower specific saturation magnetization. This phenomenon can be attributed to the existing of a nonmagnetic layer existing on the surface of the particles. The higher value of the coercivity force is obtained when the particle sizes approximately are equal to 90 nm and assume a single-domain character.

Acknowledgement

This project was supported by the Doctoral Foundation of the State Education Committee of China and the Foundation of Natural Science of Jiangsu province.

References

1. G. M. WHITESIDES, J. P. MATHIAS and C. T. SETO, *Science* **254** (1991) 1312.
2. Y. WANG, *Acc. Chem. Res.* **24** (1991) 133.
3. E. M. CHUDNOVSKY and L. GUNTHER, *Phys. Rev. Lett.* **60** (1988) 661.
4. C. KITTEL, *Phys. Rev.* **70** (1946) 965.
5. E. M. CHUDNOVSKY and L. GUNTHER, *Phys. Rev. B* **37** (1988) 9455.
6. D. D. AWSCHALOM and D. P. DIVINCENZO, *Phys. Today* **48** (1995) 43.
7. A. AHARONI, "Introduction to the theory of Ferromagnetism" (Oxford University Press, New York, 1996) p. 92.
8. R. D. MCMICHAEL, R. D. SHULL, L. J. SWARTZENDRUBER and L. H. BENNETT, *J. Magn. Magn. Mater.* **111** (1992) 29.

9. Z. YANG, H. X. ZENG, D. H. HAN, J. Z. LIU and S. L. GENG, *ibid.* **115** (1992) 77.
10. P. GORNERT, E. SINN and W. SCHUPPEL, *IEEE Trans. Magn.* **26** (1990) 12.
11. C. H. LIN, Z. W. SHIN, M. L. WANG and Y. C. YU, *ibid.* **26** (1990) 15.
12. V. V. PANKOV, M. PERNET, P. GERMI and P. MOLLARD, *J. Magn. Magn. Mater.* **120** (1993) 69.
13. F. LECCABUE, O. ARES-MUZIO, M. S. E. KANY, G. CALESTANI and G. ALBANESE, *ibid.* **68** (1987) 201.
14. F. LICCI and T. BESAGNI, *IEEE Trans. Magn.* **MAG-20** (1984) 1639.
15. J. RIVAS, M. A. LOPEZ-QUINTELA, J. A. LOPEZ and L. LIZ, *IEEE Trans. Magn.* **29** (1993) 2655.
16. V. PILLAI, P. KUMAR and D. O. SHAH, *J. Magn. Magn. Mater.* **166** (1992) L299.
17. A. SRIVASTAVA, P. SINGH and M. P. GUPTA, *J. Mater. Sci*. **22** (1987) 1489.
18. V. K. SANKARANARAYANAN, Q. A. PANKHURST, D. P. E. DICKSON and C. E. JOHNSON, *J. Magn. Magn. Mater.* **120** (1993) 73.
19. X. H. WANG, G. XIONG, X. WANG, L. D. LU and X. J. YANG, *ibid.* **189** (1998) 96.
20. X. H. WANG, G. XIONG and X. WANG, *J. Mater. Sci. Lett.* **16** (1997) 1606.
21. L. S. BIRKS and H. J. FRIEDMAN, *Appl. Phys.* **17** (1946) 687.
22. G. XIONG, Z. L. ZHI, X. J. YANG, L. D. LU and X. WANG, *J. Mater. Sci. Lett.* **16** (1997) 1064.
23. O. KUBO, T. IDO, H. YOKOYAMA and Y. KOIKE, *J. Appl. Phys.* **57** (1985) 4280.
24. G. HERZER, *Mater. Sci. & Eng. A.* **133** (1991) 1.

Received 15 January
and accepted 22 July 1999